GLOBAL BIOGEOCHEMICAL CYCLES, VOL. 14, NO. 2, PAGES 573-584, JUNE 2000

Mean annual cycle of the air-sea oxygen flux: A global view

Raymond G. Najjar[1]
Department of Meteorology, Pennsylvania State University, University Park

Ralph F. Keeling
Scripps Institution of Oceanography, La Jolla, California

Abstract. A global monthly-mean climatology of the air-sea oxygen flux is presented and discussed. The climatology is based on the ocean oxygen climatology of *Najjar and Keeling* [1997] and wind speeds derived from a meteorological analysis center. Seasonal variations are characterized by outgassing of oxygen during spring and summer and ingassing of oxygen during fall and winter, a pattern consistent with thermal and biological forcing of the air-sea oxygen flux. The annual mean flux pattern is characterized by ingassing at high latitudes and the tropics and outgassing in middle latitudes. The air-sea oxygen flux is shown to exhibit patterns that agree well with patterns seen in a marine primary productivity climatology, in model generated air-sea O_2 fluxes, in estimates of remineralization in the shallow aphotic zone based on seasonal oxygen variations, in observed seasonal nutrient-temperature relationships, and in independent estimates of meridional oxygen transport in the Atlantic ocean. We also find that extratropical mixed layer new production during the spring-summer period, computed from biological seasonal net outgassing of oxygen, is equivalent to the production of 4.5-5.6 Gt C, much lower than previous estimates based on atmospheric O_2/N_2 measurements.

1. Introduction

Even though the annual cycle is the dominant form of variability in many marine biogeochemical systems, global-scale descriptions of the annual cycle exist for only a small number of biogeochemically relevant variables in the ocean: chlorophyll [*Yoder et al.*, 1993; *Banse and English*, 1994], primary productivity [*Antoine et al.*, 1996], CO_2 and its air-sea flux [*Takahashi et al.*, 1997], and dissolved oxygen [*Levitus and Boyer*, 1994a; *Najjar and Keeling*, 1997]. Here we extend this list to include the air-sea oxygen flux, which is important because it can be used to infer rates of marine new primary production (the excess of photosynthesis over respiration in the euphotic zone), a process that generates many chemical gradients in the sea and represents the amount of nutrients required to keep euphotic zone ecosystems from running down [*Dugdale and Goering*, 1967]. Knowledge of the air-sea O_2 flux can also help to place constraints on the biological and physical processes that control air-sea exchanges of CO_2. A better understanding of such exchanges is needed to reduce uncertainties in the atmospheric CO_2 budget [e.g., *Tans et al.*, 1990]. Finally, the air-sea oxygen flux climatology should also be a valuable data set for evaluating large-scale marine biogeochemical models.

The air-sea flux climatology is essentially that used by *Keeling et al.* [1998], which is based on separate climatologies of the surface ocean oxygen anomaly [*Najjar and Keeling*, 1997] and the air-sea gas transfer velocity for oxygen. Atmospheric general circulation model (GCM) simulations of the seasonal, oceanic component of the atmospheric O_2/N_2 ratio forced by these oxygen flux fields gave excellent results, providing a validation of the fluxes integrated over large scales, particularly in middle and high latitudes [*Keeling et al.*, 1998; *Maloit*, 1998]. It is important to keep in mind that the GCM calculations reveal a level of certainty in the oxygen flux that is greater than the certainty of the oxygen anomaly and gas transfer velocity from which it was derived.

2. Air-Sea Oxygen Flux Computation

The flux fields presented here differ from those of *Keeling et al.* [1998] in that we explicitly treat bubble-induced supersaturation and we use slightly different heat flux and wind speed data to compute the skin temperature correction for the oxygen anomaly. The differences, however, are very minor and do not affect the conclusions of this study or those of *Keeling et al.* [1998]. The total air-sea O_2 flux is taken to be the product of the gas transfer velocity (k_w) and the oxygen anomaly ($\Delta[O_2]$). The transfer velocity is based on the formulation of *Wanninkhof* [1992] for long-term winds, set to zero in ice-covered regions given by the atlas of *Shea et al.* [1992]. We chose the *Wanninkhof* [1992] formulation because it appears to be more suited to large-scale applications than the formulation of *Liss and Merlivat* [1986], as noted by *Keeling et al.* [1998]. The oxygen anomaly was computed from

$$\Delta[O_2] = \Delta[O_2]^\circ + \delta_p + \delta_T - \Delta[O_2]_{bub} + \delta, \quad (1)$$

where $\Delta[O_2]^\circ$ is the oxygen anomaly computed at one atmosphere pressure and the temperature of bulk surface water, δ_p is the adjustment for sea level pressure variations, δ_T is the adjustment for the skin temperature of the ocean, $\Delta[O_2]_{bub}$ is the oxygen anomaly caused by bubble injection, and δ is a constant deter-

[1]Also in the Department of Geoscience, Pennsylvania State University, University Park.

Copyright 2000 by the American Geophysical Union.

Paper number 1999GB900086.
0886-6236/00/1999GB900086$12.00

mined such that the global mean oxygen flux is approximately equal to zero. The δ_p is from *Keeling et al.* [1998]. $\Delta[O_2]^\circ$ is from *Najjar and Keeling* [1997], with an additional adjustment based on sea surface temperature (SST), applied to account for possible biases due to undersampling.

Here δ_T was computed according to

$$\delta_T = [O_2]^\circ_{sat}(T_{bulk}, S) - [O_2]^\circ_{sat}(T_{skin}, S), \quad (2)$$

where $[O_2]^\circ_{sat}$ is the saturation oxygen concentration from *Garcia and Gordon* [1992], T_{bulk} is the bulk temperature, T_{skin} is the skin temperature and S is the surface salinity. T_{bulk} and S were taken from the monthly mean climatologies of *Levitus and Boyer* [1994b] and *Levitus et al.* [1994], respectively. T_{skin} was computed from wind speed and surface heat flux from *Gibson et al.* [1997], and T_{bulk} was computed using the formulation of *Hasse* [1971] and constants appropriate to a sampling depth of 2.5 m. Wind speed and surface heat flux were taken from the European Center for Medium-range Weather Forecasting [*Gibson et al.*, 1997]. In ice-covered areas, δ_T was set equal to zero.

We derive $\Delta[O_2]_{bub}$ from the air-injection model of *Spitzer and Jenkins* [1989], which appears to give reasonable results for the seasonal timescales and open ocean conditions of interest here. To compute the injection flux, F_{inj}, with this model, the ratio of the O_2 diffusivity to the diffusivity of He at 20°C is required. We use the Schmidt number (Sc) ratio instead, taking Sc for O_2 from *Keeling et al.* [1998] and Sc for He from *Wanninkhof* [1992]. F_{inj} depends nonlinearly on wind speed and so the injection flux computed under variable winds will be different from the injection flux computed from a constant wind. Since F_{inj} goes as approximately the square of the wind speed, we multiply F_{inj} by 1.26, following *Wanninkhof*'s [1992] analysis of the wind speed probability distribution over the ocean. $\Delta[O_2]_{bub}$ is simply F_{inj}/k_w.

With $\delta = 0$, the global mean oxygen flux is computed to be 1.3 mol m^{-2} yr^{-1} into the ocean. Though there may be a net flux of oxygen into the ocean that balances the riverine input of organic carbon, we estimate this to be very small. Estimates of organic C delivery to the ocean are of the order of 0.3 Gt C yr^{-1} [*Sarmiento and Sundquist*, 1992]. Using an O_2:C ratio of 1.45 [*Anderson and Sarmiento*, 1994], this would correspond to an oceanic sink of O_2 of ~ 0.1 mol m^{-2} yr^{-1}. Thus we believe that the global mean flux computed from our flux maps is incorrect, possibly due to a systematic bias in the oxygen measurements or the correction terms. We set $\delta = 0.7$ μmol kg^{-1}, which is the value required to bring the global mean O_2 flux to approximately zero.

To determine the relative importance of biological and thermal forcing on the air-sea oxygen flux, we computed the thermally induced oxygen flux according to *Keeling et al.* [1993]:

$$F_T = -\frac{\partial [O_2]^\circ_{sat}}{\partial T}\frac{Q}{C_p}, \quad (3)$$

where Q is the total air-to-sea flux of heat, taken from *Gibson et al.* [1997], and C_p is the specific heat of seawater, taken to be constant at 3993 J kg^{-1} K^{-1}. In ice-covered waters, we set F_T equal to zero since heat flux related to sea ice freezing and melting does not induce temperature changes, which are needed to generate a

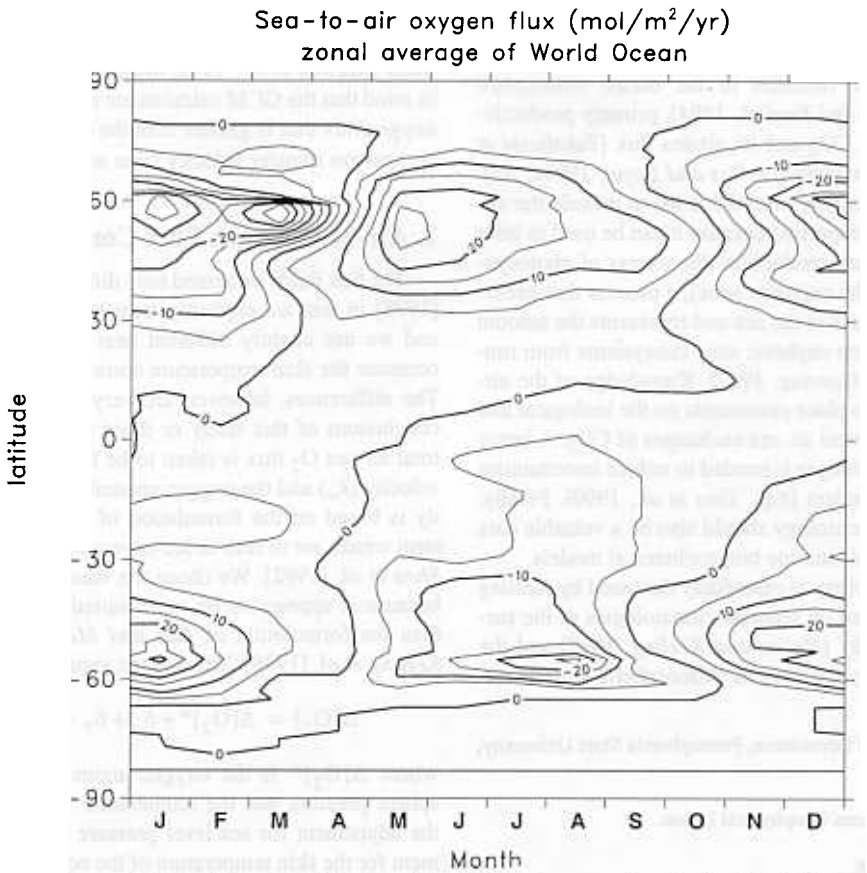

Figure 1. Zonal average of the monthly sea-to-air oxygen flux for the World Ocean

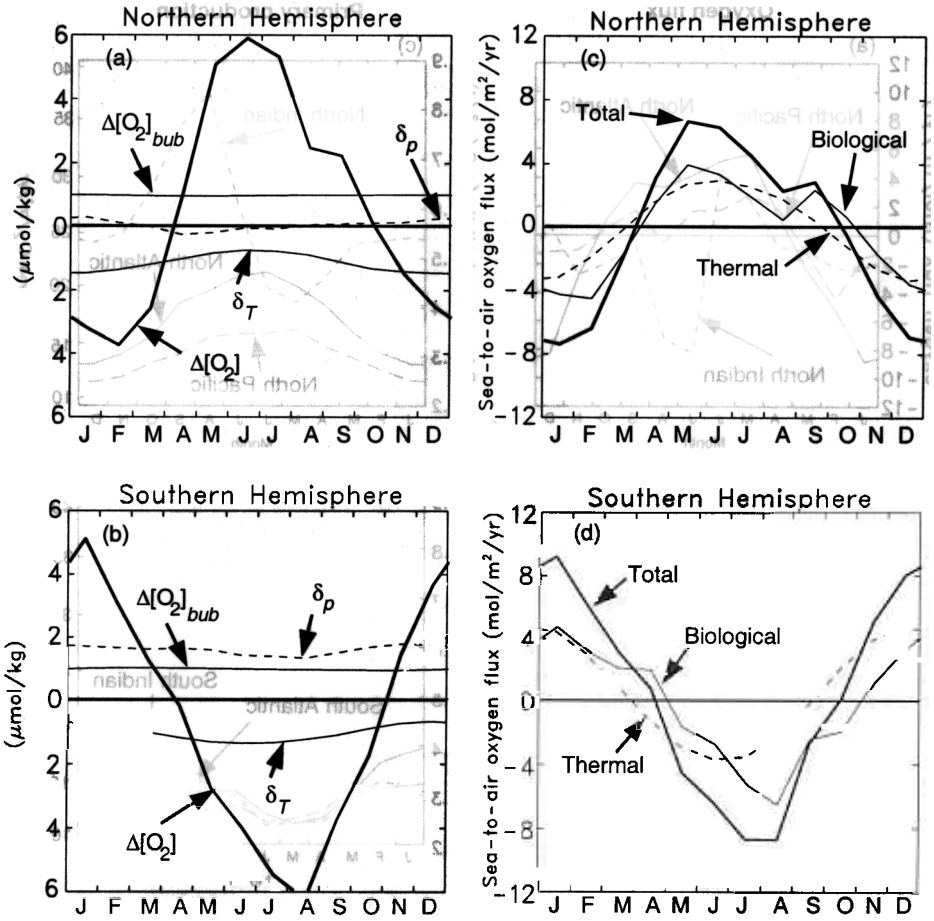

Figure 2. Seasonal variations of Northern and Southern Hemispheric averages of (a and b) the surface ocean oxygen anomaly ($\Delta[O_2]$) and the individual adjustments for skin temperature (δ_T), sea level pressure (δ_p), and bubbles ($\Delta[O_2]_{bub}$) and (c and d) the total, thermal, and biological sea-to-air oxygen flux. Averages include ice-covered waters.

thermal oxygen flux. We then computed the biologically induced oxygen flux (F_B) as the total flux minus F_T.

All of the terms on the right-hand side of (1) were computed in terms of μmol kg^{-1} and converted to mol m^{-3} using a constant seawater density of 1025 kg m^{-3}. All of the calculations were carried out on the nearly equal-area grid of *Najjar and Keeling* [1997], which is 2° × 2° at the equator. Calculations are made for each month of the year using monthly-mean values for all inputs.

3. Results and Discussion

3.1. Seasonal Variations

We begin the discussion of the results with the zonally averaged air-sea oxygen flux for the World Ocean, shown in Figure 1. Oxygen is released to the atmosphere during the spring and summer and taken up by the ocean during the fall and winter in both hemispheres, consistent with thermal and biological forcing of the flux associated with seasonal variations in mixed layer depth [*Najjar and Keeling,* 1997]. Along the equator, the annual cycle follows that of the Southern Hemisphere with a lag of several months. Examination of individual basins (not shown) reveals that the equatorial cycle is dominated by the eastern Pacific and is consistent with upwelling of cold, oxygen-depleted water, as revealed by seasonal variations in the eastern equatorial Pacific cold tongue [*Wyrtki,* 1981]. The greatest seasonal variability occurs between 50° and 60° latitude in both hemispheres. Despite increasing seasonal variations of the oxygen anomaly poleward of 50°-60° latitude in both hemispheres [*Najjar and Keeling,* 1997], seasonal variations in the flux decrease because of decreases in the transfer velocity associated with increased sea ice extent and decreased wind speeds.

Figures 2a and 2b show hemispheric averages of the surface oxygen anomaly and the sea level pressure, skin temperature, and bubble adjustments in ice-free waters. The seasonal amplitude of the hemisphere-averaged oxygen anomaly is slightly larger in the Southern Hemisphere. Seasonal variations in the pressure and skin temperature adjustments, although small, are not insignificant. $\Delta[O_2]_{bub}$ has little seasonal variation because F_{inj} and k_w have similar dependencies on SST and wind speed. The hemisphere-averaged sea-to-air oxygen flux (Figure 2c and 2d) generally mimics the hemisphere-averaged oxygen anomaly, both being positive in the spring and summer, and negative in the fall and winter. In the Northern Hemisphere, the seasonally asymmetry seen in the anomaly is absent in the flux because of counteracting seasonal variations in the transfer velocity. The seasonal variations in the

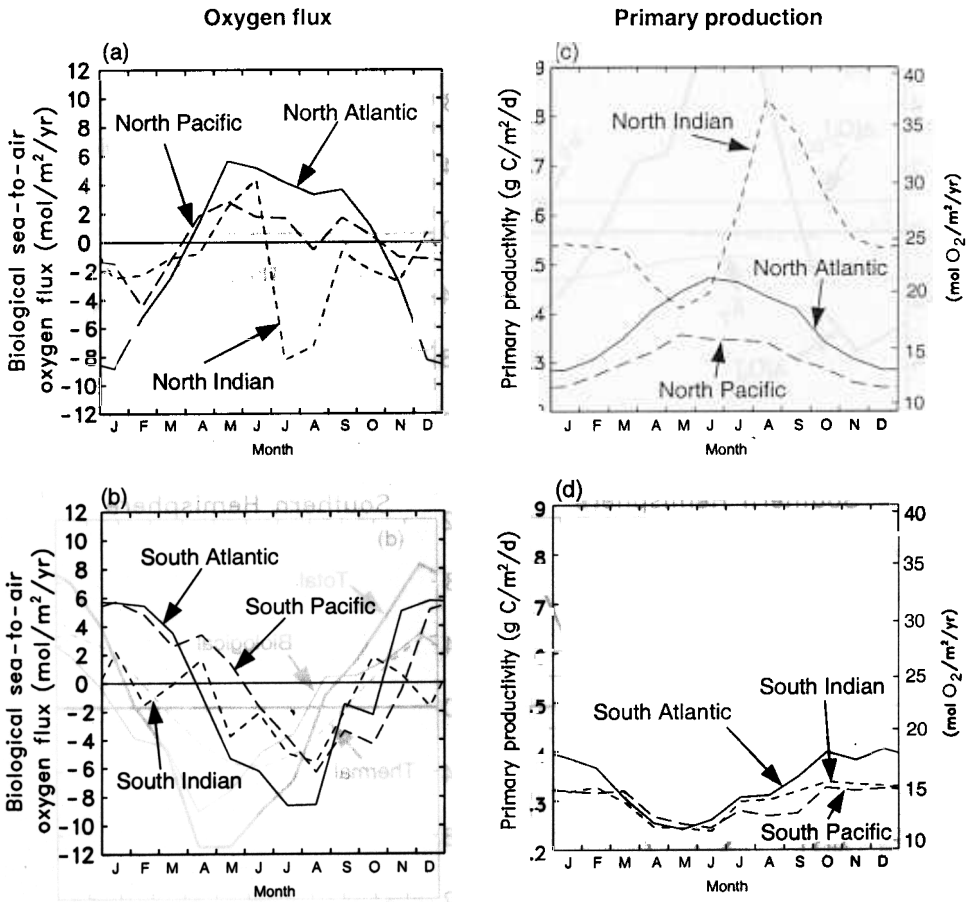

Figure 3. Seasonal variations of averages over each of the major ocean basins of (a and b) the biological sea-to-air oxygen flux and (c and d) satellite-based primary productivity estimated by *Antoine et al.* [1996] for individual ocean basins in the Northern (Figures 3a and 3c) and Southern Hemispheres (Figures 3b and 3d). Averages of the biological oxygen flux include ice-covered waters. The conversion from carbon to oxygen for primary production used an O_2:C ratio of 1.45 [*Anderson and Sarmiento,* 1994].

hemisphere-averaged flux are greater in the Southern Hemisphere than in the Northern Hemisphere, unlike the zonal averages, because the zone of maximum seasonal variation (between 50° and 60° latitude) is a larger fraction of the hemispheric area in the Southern Hemisphere.

In each hemisphere, the average thermal oxygen flux leads and has a somewhat smaller amplitude than the average biological oxygen flux. The lead may be more apparent than real because full equilibration has been assumed in computing the thermal oxygen flux using (3). The amplitude of the thermal oxygen flux is slightly overestimated for the same reason, and so the amplitude of the biological oxygen flux is slightly underestimated.

The pattern of seasonal variation in the biological oxygen flux is similar among all of the major ocean basins (Figures 3a and 3b), mimicking the hemispheric pattern (Figure 2), with the exception of the North Indian Ocean, which departs from the other basins in the summer with a large influx of oxygen. This reflects the presence of the Asian summer monsoon, which causes coastal and open ocean upwelling as well as vertical mixing [*Bauer et al.,* 1991] that bring oxygen-depleted waters to the surface.

The patterns of the amplitude and phasing of the seasonal O_2 cycles are similar to the patterns seen in primary productivity determined from space (Figures 3c and 3d) by *Antoine et al.* [1996]. Ocean basins with greater primary productivity tend to have larger amplitudes of the annual cycle in the biological oxygen flux. For example, the North Atlantic has a higher primary productivity and a greater amplitude in the annual cycle of the biological oxygen flux than the North Pacific. A similar difference is seen between the South Atlantic and South Pacific, though the South Indian does not fit this trend. Differences between hemispheres also do not seem to fit this trend. The distinctive character of the North Indian Ocean shows up in the oxygen flux and the primary productivity in a consistent fashion: The period of strong oxygen influx to the ocean coincides with the period of upwelling and intense vertical mixing of nutrients, which results in high primary productivity.

3.2. Seasonal Net Outgassing

3.2.1. Comparison to *Keeling and Shertz* [1992]. *Keeling and Shertz* [1992], hereafter KS, define seasonal net outgassing (SNO) as the areally and temporally integrated flux of O_2 from the ocean to the atmosphere over the spring/summer period, when the areally integrated flux is upward. They computed the biological

Table 1. Biological and Thermal SNO for the Northern and Southern Hemispheres.

	Biological SNO			Thermal SNO	
	This work	calibrated[a]	KS[b]	ECMWF	KS[b]
NH	1.90	2.23	4.6	1.54	1.56
SH	3.23	4.03	6.8	2.87	1.80
Total	5.13	6.26	11.4	4.41	3.36

SNO is given in 10^{14} mol O_2. NH, Northern Hemisphere; SH, Southern Hemisphere.

a. Fluxes without bubble correction increased poleward of 30° latitude following *Keeling et al.* [1998].

b. *Keeling and Shertz* [1992].

component of SNO in both the Northern and Southern Hemispheres from seasonal variations in the atmospheric O_2/N_2 ratio, from estimates of air-sea heat fluxes, and from two assumptions about atmospheric mixing: (1) there is insignificant interhemispheric mixing on the seasonal timescale and (2) mixing within each hemisphere is such that the seasonal increase in atmospheric oxygen at the surface stations is about twice what would be expected if the air in one hemisphere were well mixed.

We computed biological SNO from the hemisphere-averaged biological oxygen flux (Figures 2c and 2d) by first subtracting off the (small) annual mean flux from each monthly value and then integrating the flux over the months in which the flux is upward. Thermal SNO was computed in the same fashion. The comparison with KS is shown in Table 1. Our estimates of biological SNO are 39 and 46% of those of KS in the Northern and Southern Hemispheres, respectively. Part of the discrepancy may be due to the underestimate (15% in the Northern Hemisphere and 23% in the Southern Hemisphere) of the seasonal variations in the flux fields poleward of 30° latitude, as found by *Keeling et al.* [1998]. However, if the total fluxes (without the bubble correction, as in *Keeling et al.* [1998]) are accordingly increased poleward of 30° latitude, our SNO estimates are still much lower than those of KS: 48% of KS in the Northern Hemisphere and 59% of KS in the Southern Hemisphere.

The difference in the Northern Hemisphere can be partly explained by different weighting given to the observations at La Jolla by KS and *Keeling et al.* [1998]. La Jolla was only one of two stations available to KS in the Northern Hemisphere and was taken to be representative of midlatitude stations in their Northern Hemisphere estimate. In contrast, the results from La Jolla were ignored in the more recent study by *Keeling et al.* [1998] in favor of three other stations in the Northern Hemisphere. The results from La Jolla were ignored on the grounds that the sampling strategy used probably leads to an upward bias in the seasonal amplitude that is not reproduced in the atmospheric transport model and on the grounds that the model could not be adjusted to yield simultaneous agreement at La Jolla and any of the other three selected Northern Hemisphere stations. The discrepancy at La Jolla therefore probably does not indicate problems with the air-sea flux maps so much as indicating that the La Jolla results are not characteristic of midlatitudes in the Northern Hemisphere, in contrast to the assumption of KS.

Another factor contributing to differences in our SNO estimates from KS are estimates of thermal SNO in the Southern Hemisphere. Ours is 59% higher than that of KS and accounts for ~25% of the discrepancy in biological SNO in the Southern Hemisphere. This difference is due to the large difference in the heat fluxes used to compute thermal SNO. The amplitude of the annual cycle in heat flux estimated from the meteorological analyses (used here) is much larger than that inferred from the storage of heat computed from hydrographic data (used by KS).

A final factor, probably the most important, is that the transport model calculations of *Keeling et al.* [1998] require somewhat smaller SNO to account for the seasonal atmospheric O_2/N_2 increase than assumed by KS. KS assumed that the effective dilution in the atmosphere of the oxygen outgassed from the ocean could be estimated based on an analogy with the annual cycle of atmospheric CO_2 in the Northern Hemisphere, which is driven largely by exchanges with land biota. The situation is not strictly analogous, however, because most of the observation stations (for both CO_2 and O_2/N_2) are located in the marine boundary layer, where a gas flux of terrestrial origin will result in a smaller concentration change than the same flux of oceanic origin.

3.2.2. New production and the *f* ratio. As has been frequently suggested, the biological sea-to-air oxygen flux should closely approximate new production within the mixed layer during the shoaling period [*Jenkins and Goldman,* 1985; *Emerson,* 1987; *Keeling and Shertz,* 1992; *Bender et al.,* 1996]. Here we estimate spring-summer new production for 10° latitude bands in each major ocean basin using the biological air-sea oxygen flux. Because much of the new production in tropical regions is advectively driven and not reflected in biological SNO, we do not include the North Indian Ocean and regions equatorward of 20° latitude. Biological SNO for each of the zones was computed in a manner exactly analogous to the computation of hemispheric SNO: We spatially averaged the flux in each zone for each month, subtracted off the annual mean, and then added up the positive monthly values. These calculations were done without increasing the middle-high latitude fluxes to agree with atmospheric O_2/N_2 variations. The result is shown in Figure 4.

For comparison, we have also plotted an estimate of the vertically integrated remineralization rate in the shallow aphotic zone, which was calculated as follows. First, the mean annual cycle of the oxygen anomaly of *Najjar and Keeling* [1997] was averaged over 12° latitude bands in each basin at each depth. Second, an annual harmonic was fit to each annual cycle. Finally, the peak-to-trough amplitude of this fit was vertically integrated between the oxygen nodal depth, which should approximate the community compensation depth [*Najjar and Keeling,* 1997], and 450 m. No attempt has been made to "scale up" the amplitudes of the deep oxygen cycles to reflect undersampling. As $\Delta[O_2]$ generally decreases throughout the spring and summer in the aphotic zone, this calculation is an estimate of remineralization during this time period. Assuming this remineralization represents the decomposition of organic matter exported from the euphotic zone above, it should be equivalent to new production. The equivalence is not strictly valid because of dissolved organic carbon (DOC) transport, which can decouple production at a given location from the remineralization directly below. But DOC export is thought to account for only ~ 20% of new production globally [*Hansell and Carlson,* 1998]. Further, this DOC has a lifetime of only ~ 2 months [*Archer et al.,* 1997], which would prohibit transport over great horizontal distances.

In general the two estimates of new production (outgassing and aphotic zone oxygen decrease) integrated over the spring and sum-

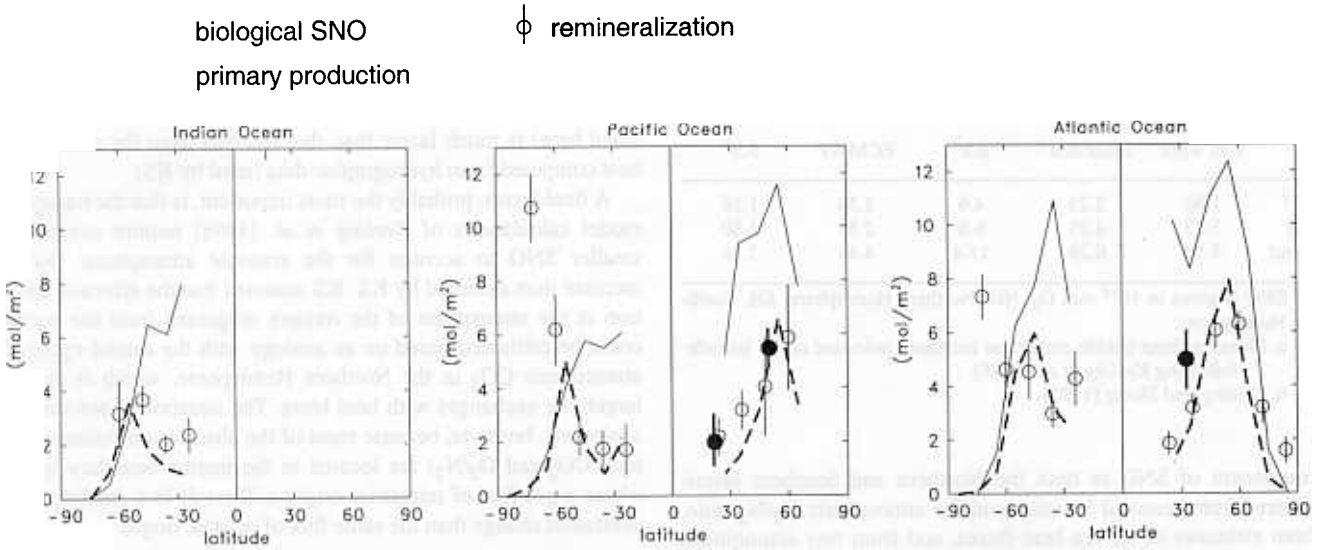

Figure 4. Biological SNO, primary production during the outgassing period, and vertically integrated remineralization as a function of latitude, poleward of 20° latitude, and excluding the North Indian Ocean. See text for computation of biological SNO and primary production. Remineralization was computed by vertically integrating the amplitudes of the annual cycle of the average oxygen anomaly in 12° latitude bands from the climatology of *Najjar and Keeling* [1997]. The integration is from the oxygen nodal depth to 450 m. The nodal depth was taken to be 40 m poleward of 66° latitude, 62.5 m between 42° and 66° latitude, and 87.5 m between 18° and 42° latitude. The error is the weighted quadrature sum of the RMS error of the annual harmonic fit. New production estimates of *Jenkins and Goldman* [1985], *Emerson et al.* [1991, 1997] are indicated by solid circles.

mer correspond well with each other, except in the high southern latitudes of the Atlantic and Pacific Oceans, where the outgassing is much smaller than the remineralization. The difference may suggest that a greater fraction of new production at high latitudes is stored in the ocean as opposed to outgassed, possibly owing to ice cover limiting air-sea gas transfer. The estimates of new production of the oxygen climatology are also in reasonable agreement with those made at individual sites in the subtropical North Pacific [*Emerson et al.*, 1997], the subtropical North Atlantic [*Jenkins and Goldman,* 1985] and the subarctic North Pacific [*Emerson et al.*, 1991].

The favorable agreement of biological SNO with remineralization estimates and site-specific new production estimates encourages us to use it make larger-scale estimates of new production. Adding up the individual 10° latitude bands leads to a global estimate of extratropical spring-summer mixed layer new production of 540 Tmol O_2 (1 Tmol = 10^{12} mol), or 4.5 Gt C, using an O_2:C ratio of 1.45. If we scale up the O_2 fluxes following *Keeling et al.* [1998], we find that these values increase to 670 Tmol O_2 and 5.6 Gt C. These estimates are somewhat lower than the 6.6±0.4 Gt C determined by integrating the remineralization estimates presented in Figure 4. The difference may be due to production in the seasonal thermocline, which is not reflected in SNO but which contributes to aphotic zone remineralization.

We can compare the estimate of new production based on biological SNO to a corresponding estimate of primary production based on the analysis of satellite observations by *Antoine et al.* [1996]. Using their analyses, we have computed primary production averaged over 10° latitude bands in each basin, integrated over the same months over which biological SNO was computed; these are also plotted in Figure 4. The pattern of primary production generally mimics that of biological SNO poleward of 20° latitude. Clearly, however, a greater fraction of primary production is new in high latitudes compared to middle latitdues. Spatially integrating the seasonal primary production in the same way as the biological SNO yields a value of 11.8 Gt C for the extratropical mixed layer, and thus an *f* ratio of 0.38-0.46.

3.2.3. Coastal versus open-ocean biological SNO. It has been suggested that a disproportionate fraction of new production occurs in coastal waters, where primary production and *f* ratios are high [*Eppley and Peterson,* 1979]. It might therefore be expected that biological SNO has a coastal bias as well. To check this, we computed the fraction of biological SNO that occurs in coastal waters, defined by those grid points whose mean depth is less than 600 m (13% of the ocean area in the Northern Hemisphere (NH) and 5% in the Southern Hemisphere (SH), on our grid). We found that the percent SNO that is coastal is approximately equal to the fractional area (14% in the NH and 5% in the SH), revealing no coastal bias. There are several possible explanations of this paradox. It may be that the O_2 flux maps do not properly resolve coastal waters or that strong vertical mixing in coastal waters prevents a large export of organic carbon from the mixed layer, which is required in order to produce SNO. It is also possible that coastal new production has been overestimated.

3.2.4. Relationship between thermal and biological SNO. The thermal and biological components of the air-sea oxygen flux are correlated not only temporally (Figure 2) but also spatially. This is seen in Figure 5, a plot of biological SNO as a function of thermal SNO in 10° latitude bands in all of the major ocean basins (except the North Indian Ocean) poleward of 20° latitude. Such a relationship is expected if, as *Keeling et al.* [1993] speculated, the biological air-sea oxygen flux is related to the heat flux on the sea-

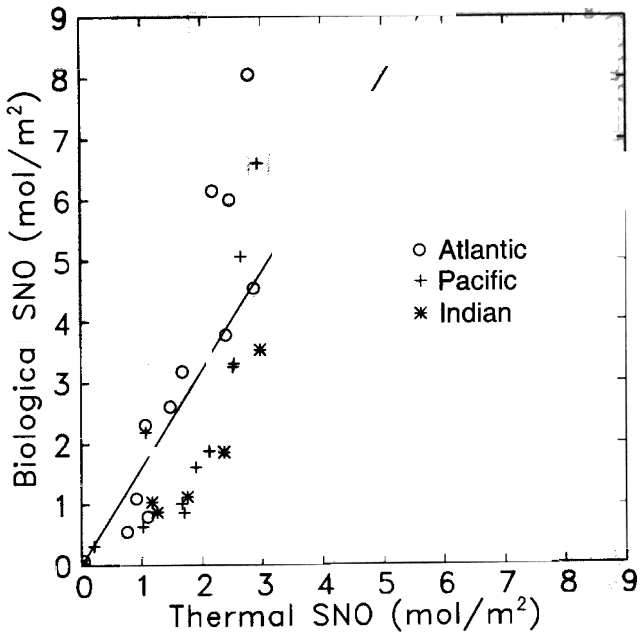

Figure 5. Scatterplot of biological SNO as a function of thermal SNO averaged over 10° latitude bands poleward of 20° latitude in all of the major ocean basins except the North Indian Ocean. The line is a visual fit to the data and has a slope of 1.6.

sonal time frame. On the basis of observed nutrient-temperature relationships, *Takahashi et al.* [1993] suggested that biological (new) production and heat flux were linked because solar radiation drives both processes. A relationship between heat flux and new production is also expected on the seasonal timescale because a large seasonality in heat flux implies a large seasonality in mixed layer depth, which causes a large entrainment of nutrients into the euphotic zone. Here we see to what extent the relationship between the latitudinal patterns in thermal and biological SNO is consistent with observed phosphate-temperature relationships.

Mixed layer new production during the shoaling period can be expressed as

$$P = h\frac{d[PO_4]}{dt} = \frac{F_B}{r}, \quad (4)$$

where P has units of mol P m^{-2} s^{-1}, h is the mixed layer depth, $[PO_4]$ is the mixed layer phosphate concentration, F_B is the biological air-sea oxygen flux, and r is the O_2:P Redfield ratio. The corresponding mixed layer heat balance for the shoaling period is

$$Q = hC_p\frac{dT}{dt} \quad (5)$$

Combining the last two equations with (3) leads to the following estimate of the phosphate-temperature relationship in the mixed layer:

$$\frac{d[PO_4]}{dT} = \frac{1}{r}\frac{d[O_2]_{sat}}{dT}\frac{F_B}{F_T}. \quad (6)$$

Taking values of 170 for r [*Anderson and Sarmiento,* 1994], 6 μmol O_2 kg^{-1} K^{-1} for the second term (the average between 0 and 20°C), and 1.6 for F_B/F_T (Figure 5), we arrive at phosphate-temperature relationship of 0.06 μmol P kg^{-1} K^{-1}. *Takahashi et al.* [1993], in their comprehensive study of middle and high latitude surface waters in all of the major ocean basins, found phosphate-temperature slopes of 0.05-0.11 μmol P kg^{-1} K^{-1}, with little seasonal variation. Our estimate is at the low end of this range, and we expect this for two reasons. First, biological SNO has been underestimated because of the overestimate of thermal SNO, as discussed earlier. Second, the biological O_2 flux most consistent with atmospheric O_2/N_2 cycles should be slightly increased poleward of 30° latitude.

3.3. Annual Mean Fluxes

We now turn to the annual mean air-sea oxygen fluxes, as shown in Figure 6 for each of the major ocean basins, along with the thermal and biological components of the flux. Although the thermal component of the flux is significant, the overall pattern of the total flux is dominated by the biological component. The total flux averaged over the World Ocean (Figure 6a), which is dominated by the Pacific, is roughly symmetric about the equator, with oxygen entering the ocean in subpolar (~60°) and equatorial latitudes and leaving the ocean in middle latitudes. A distinct double peak is apparent in middle latitudes with maxima at ~ 45°-50° and 15°-20°. The pattern of the zonally averaged annual-mean oxygen flux generally reflects the corresponding pattern of the surface oxygen anomaly (Figure 7), which includes significant adjustments for sea level pressure variations, bulk-skin temperature differences, and bubble injection.

Following the interpretation of marine biogeochemical models of *Stephens et al.* [1998], we can qualitatively explain the World Ocean zonal mean biological oxygen flux largely from the wind-driven Ekman circulation. Nutrient-rich, oxygen-depleted water upwells near the equator and in subpolar waters causing an influx of oxygen from the atmosphere. In high latitudes, convection also contributes to the upward flux of oxygen-depleted water. As the water travels toward the subtropics, oxygen absorbed from the atmosphere and oxygen produced from new production brings surface waters close to equilibrium with the atmosphere. As the waters continue toward the center of downwelling in the subtropics, new production continues, causing waters to become supersaturated. Some of the new nitrogen is probably also supplied by eddy-pumping and nitrogen fixation [*Falkowski et al.,* 1991; *Capone et al.,* 1997]. As nutrients become very low in the subtropics, however, new production slows, and air-sea transfer of oxygen brings surface waters close to equilibrium again. These waters downwell in the subtropics with very low nutrient content and close the cycle by travelling meridionally in the aphotic zone, increasing their nutrient content and decreasing their oxygen content.

There are a number of interesting differences in the annual mean flux between the major ocean basins (Figure 6b-6d). The influx in the high northern latitudes is much more intense in the Atlantic than in the Pacific, consistent with the difference in thermohaline circulation between the two oceans. Deep water formation, which is present in the North Atlantic but not the North Pacific, causes a large thermal influx of oxygen from the atmosphere. Similarly, deep convection in the North Atlantic creates a biological influx by bringing deep, oxygen-depleted water to the surface. The North Pacific shows a much smaller biological influx but a much larger efflux at around 50°N, possibly due to the productivity supported by the southward Ekman transport of high-nutrient water (characteristic of the North Pacific) across the

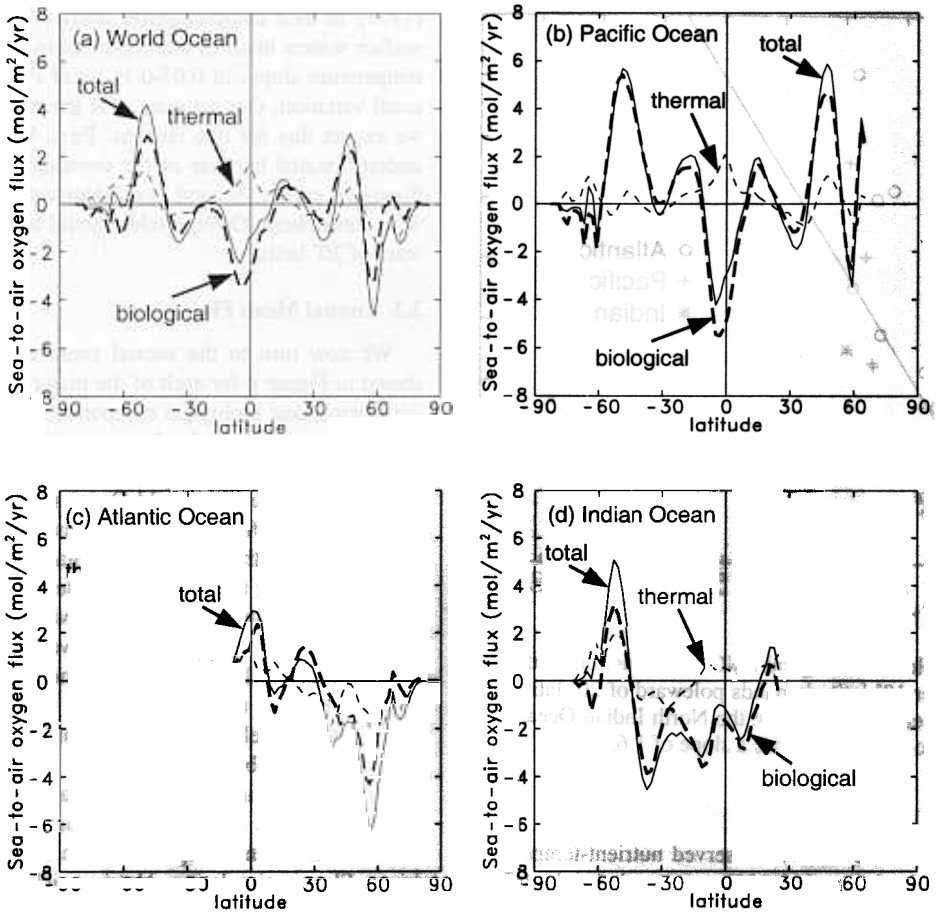

Figure 6. The zonal- and annual-mean sea-to-air oxygen flux and its thermal and biological components for the major ocean basins and the World Ocean.

boundary between the subpolar and subtropical gyres. At the equator, there is an efflux of oxygen from the Atlantic Ocean and an influx into the Pacific ocean. The equatorial Pacific influx likely reflects upwelling of oxygen-depleted water. Although upwelling of cold, nutrient-rich, oxygen-poor water also occurs in the equatorial Atlantic, it does so to a much smaller degree, as evidenced by the weaker SST minimum and nutrient maximum in the equatorial Atlantic as compared to the equatorial Pacific [*Levitus and Boyer*, 1994b; *Conkright et al.*, 1994]. More to the point, it appears that nutrients that are upwelled in the equatorial Atlantic are almost completely locally utilized, thereby causing the equatorial Atlantic to be an O_2 source to the atmosphere.

Support for the annual mean flux distribution can be found in the three-dimensional marine biogeochemical models of *Stephens et al.* [1998], which provide completely independent estimates of the air-sea oxygen flux. The models and observations show the same basic pattern of minima and maxima for the World Ocean, the Atlantic, and the Pacific. Similar Pacific-Atlantic differences are present in the model and observations, including the Atlantic efflux and Pacific influx at the equator and the relatively strong influx in the subarctic Atlantic. Throughout the southern high latitudes, however, the models show a strong influx, while the observations show a weak influx or an efflux. This may reflect a problem with the models, as suggested by simulations of atmospheric potential oxygen [*Stephens et al.*, 1998], or a problem with the flux climatology, as discussed in Section 4.1 below.

3.4. Implied Meridional Oxygen Transport in the Atlantic Ocean

The annual mean air-sea oxygen flux provides a means for computing the annual mean meridional transport of oxygen in the ocean, assuming that the vertically and annually integrated biological source/sink function for oxygen is equal to zero. This assumption is valid if most of the organic matter produced in the water column is not transported across large (basin-scale) horizontal distances—such as would be the case if fast-sinking particles and semilabile dissolved organic matter dominate the downward flux of organic matter and sedimentary burial is small. From our analyses, we computed the meridional transport of oxygen in the Atlantic Ocean and compare with transport estimates made from hydrographic sections and water mass analysis [*Brewer et al.*, 1989; *Rintoul and Wunsch*, 1991; *MacDonald*, 1993; *Martel and Wunsch*, 1993; *Keeling and Peng*, 1995; *Saunders and King*, 1995]. We do not show results for other basins, where the flux maps are less certain and independent transport estimates are few. The net northward transport of oxygen in the Atlantic Ocean (north of 35°S) at a given latitude is computed by horizontally

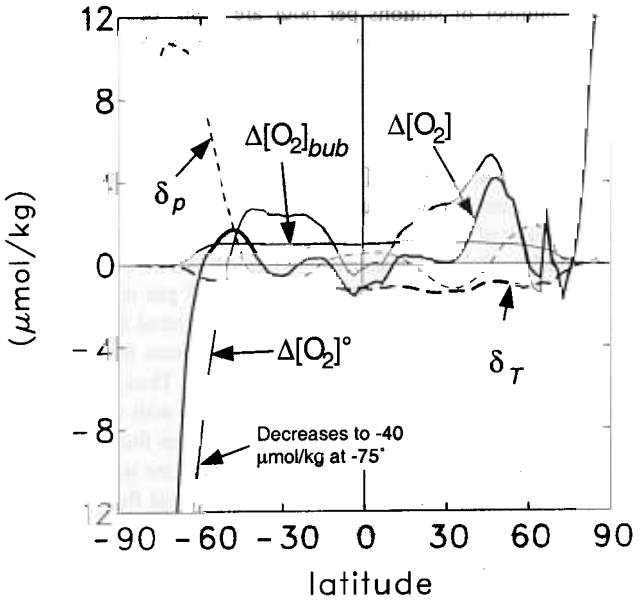

Figure 7. Zonal and annual averages of the adjustments for sea level pressure variations (δ_p) and skin temperature (δ_T), and the oxygen anomaly with ($\Delta[O_2]$) and without ($\Delta[O_2]^\circ$) the adjustments.

integrating the annual mean air-to-sea oxygen flux north of that latitude (including the Arctic Ocean). There is a component of the oxygen transport in the Atlantic due to flow through Bering Strait. Some hydrography-based estimates of the transport include this term, and we adjust them to make comparison with the air-sea flux-based estimate straightforward. We estimate the O_2 transport through Bering Strait as the product of the net flow (0.8×10^6 m^3 s^{-1} to the north [*Roach et al.*, 1995]) and the mean oxygen concentration. Because the sill depth at the strait is only 50 m, the water flowing through the strait is mainly mixed layer water which therefore has an oxygen content close to equilibrium with the atmosphere. The oxygen saturation concentration at the average temperature and salinity of Bering Strait seawater (0°C and 33 ‰ [*Roach et al.*, 1995]) is ~ 350 mmol m^{-3}. Thus there is a northward flux of oxygen through Bering Strait of ~ 9 Tmol yr^{-1}. The results of the air-sea flux computation show that the meridional oxygen transport in the Atlantic is generally to the south and in broad agreement with independent estimates of the transport based on inversion of hydrographic data and water mass analysis (Figure 8).

Although the annual mean oxygen transport at 30°N is to the south, ice-free surface waters north of this latitude in the Atlantic are supersaturated with oxygen, on average. A southward transport exists in spite of this because the transfer velocity in winter, acting on undersaturated waters, is substantially greater (due to higher wind speeds) than in summer, when surface waters are supersaturated. This point is highlighted by computing the meridional transport with different wind speed (u) dependencies of the transfer velocity (k_w), which is also shown in Figure 8. In the Wanninkhof formulation, k_w is proportional to u^2. We also computed transport with k_w proportional to u raised to powers of 0, 1, and 3 and kept the same temperature dependence. In all cases, k_w was forced through the value of k_w predicted using the Wanninkhof formulation at 7 m s^{-1}, the approximate mean wind speed over the ocean. The bubble injection flux was not changed. The results show very large sensitivity to the functional dependence of k_w on u. This finding provides additional support for the *Wanninkhof* [1992] formulation of k_w and compliments the finding by *Keeling et al.* [1998], who were able to constrain the annual mean transfer velocity for oxygen poleward of 30° latitude but not its wind speed dependence.

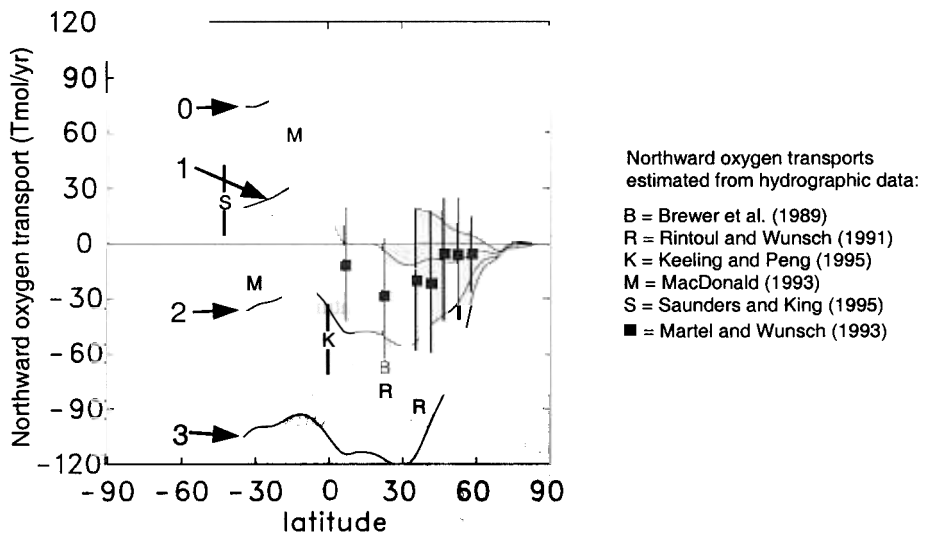

Figure 8. The meridional transport of oxygen implied by the air-sea oxygen flux in the Atlantic Ocean, along with direct estimates of the meridional transport from inversions of hydrographic data and water mass analysis. The numbers on the four curves indicate the exponent of the wind speed in the gas transfer velocity formulation. See the text for details. The southward transport driven by the flow through Bering Strait is not included in the estimate based on the air-sea flux. The transport estimates from hydrographic sections, except for those of *Martel and Wunsch* [1993] and *MacDonald* [1993], also do not include Bering Strait transport. The transports from these two studies have been increased by 9 Tmol yr^{-1} in order to be consistent with the other estimates.

4. Uncertainties and Possible Biases in the Flux Climatology

Uncertainties in the oxygen flux climatology related to sampling, bubble-induced supersaturation, short-term (submonthly) covariances between k_w and $\Delta[O_2]$, and the bulk-skin temperature difference are now discussed. Our emphasis is on the potential errors in the annual mean flux because biases in the seasonal variations have been effectively accounted for by the "calibration" of the fluxes to measurements of atmospheric O_2/N_2 [*Keeling et al.*, 1998].

4.1. Temporal Biases

There may be two temporal biases, a summertime bias and a daytime bias, in the oxygen anomaly climatology of *Najjar and Keeling* [1997] that could influence the results and interpretation of the air-sea oxygen flux given above. Because there are many regions with inadequate sampling during winter months, the objective analysis routine of *Najjar and Keeling* [1997] fills in such regions with neighboring months, causing a summertime bias in the oxygen anomaly. Generally, this means that seasonal variations will be underestimated and that the annual mean oxygen anomaly (and sea-to-air flux) will be overestimated. However, it is certain that the summertime bias is greatest in high latitudes of the Southern Hemisphere, as indicated by the SST analysis discussed *Najjar and Keeling* [1997] and *Keeling et al.* [1998]. Since surface waters in winter tend to be anomalously low in oxygen anomaly, the annual mean influx of oxygen in high latitudes has probably been underestimated, and the annual mean efflux in middle latitudes has probably been overestimated, particularly in the Southern Hemisphere. Accounting for this would bring the flux climatology in better agreement with the marine biogeochemical models discussed earlier.

There may also be a bias in the computed air-sea oxygen flux due to the diurnal cycle in the oxygen anomaly. This cycle comes about as a result of diurnal variations in SST due to surface heat flux and in oxygen due to photosynthesis and respiration. SST generally peaks in the early afternoon and is at a minimum around sunrise [*Delnore*, 1972; *Price et al.*, 1986; *Ravier-Hay and Godfrey*, 1993]. Oxygen has essentially the same phasing, though the maxima are reached in the late afternoon [*Oudot*, 1989; *Robertson et al.*, 1993]. While typical (trough to peak) amplitudes in SST are of the order of a few tenths of a degree Celsius [*Delnore*, 1972; *Price et al.*, 1986], it is not unusual to find amplitudes as high as 1°C [*Cornillon and Stramma*, 1985; *Price et al.*, 1987; *Deschamps and Frouin*, 1984] and occasionally 3°C [*Ravier-Hay and Godfrey*, 1993] when winds are very weak. Thus amplitudes in the oxygen saturation concentration can be of the order of several μmol kg^{-1}. The amplitude in the oxygen concentration can also be considerable. *Oudot* [1989] and *Robertson et al.* [1993] both found amplitudes of ~ 5 μmol kg^{-1}. We expect therefore that the oxygen anomaly could have a diurnal amplitude of 10 μmol kg^{-1}, under certain conditions, with the anomaly peaking in the midafternoon and reaching its minimum value around sunrise. Many, though not all, of the stations containing oxygen in the National Oceanographic Data Center (NODC) archives include the time of day when the cast was started. Of these, there is a clear preference for casts to begin at 0900 local time. Around this time, there are twice the number of casts per hour than there are during the least favorable time to begin a cast, 0200 local time. As the oxygen anomaly and the number of stations per hour are ~ 90° out of phase, it appears that there should be very little bias in the NODC data set due to the diurnal cycle.

4.2. Influence of Bubbles

The *Spitzer and Jenkins* [1989] model yields a global mean O_2 bubble injection flux of about 2 mol m^{-2} yr^{-1}, with seasonal variations typically of the order of ± 20% (not shown). These fluxes, as suggested by other investigators, are comparable to the biological fluxes that are of primary interest. Models of gas injection vary greatly, and no single model can capture the spatial and temporal variability in measurements of gas supersaturation in the surface ocean, sparse as those measurements might be. Thus, as noted by *Emerson et al.* [1993], until better agreement with observations can be found, "determination of the air injection flux from wind speed and empirically determined parameters alone will be a risky exercise." Here, however, our large-scale seasonal fluxes are less impacted by these uncertainties due to the constraint imposed by the atmospheric O_2/N_2 observations.

4.3. Short-Term Covariances

Using one-dimensional ecosystem models, *Keeling et al.* [1998] suggested that seasonal net outgassing and ingassing is overestimated when computed from monthly means of k_w and $\Delta[O_2]$, the reason being that high wind events drive the surface ocean toward saturation. Short-term variability, however, is much greater in the winter time, when storms are more frequent and intense. Thus it is likely that the ingassing overestimate due to ignoring short-term covariations is larger than the corresponding outgassing overestimate, leading to an overestimate of the annual mean air-to-sea oxygen flux. The overestimate would also be greater at higher latitudes, causing an overestimate of the equatorward transport of oxygen in the ocean.

4.4. Thermal Skin Correction

Using the *Hasse* [1971] formula, the oxygen skin temperature correction, δ_T, has a global mean value of ~ 1 μmol kg^{-1} and seasonal variations typically of the same magnitude. Since 1 μmol kg^{-1} translates into an air-sea oxygen flux of ~ 2 mol m^{-2} yr^{-1} (using a transfer velocity of 20 cm hr^{-1}), the skin temperature correction is not trivial. Models of the bulk-skin temperature difference vary greatly and generally make predictions that have errors as large as the signal [*Wick et al.*, 1996; *Donlon and Robinson*, 1997]. Thus we suspect the uncertainty in the air-sea oxygen flux due to the skin-temperature computation is at least 1 mol m^{-2} yr^{-1} and possibly larger.

5. Conclusions

We have presented a global climatology of the mean annual cycle of the air-sea oxygen flux constructed from separate climatologies of the surface oxygen anomaly and wind speed. In qualitative terms, we confirm a global pattern that was suggested many decades ago by *Richards* [1957, page 190], based on earlier work by *Redfield* [1948] on the annual O_2 cycle in the Gulf of Maine:

> The general ideas presented by Redfield must apply to the sea as a whole, with oxygen entering the sea surface for most of the year in polar regions and in regions where upwelling brings oxygen-deficient water to the surface, and leaving the sea surface most of the year in the

tropics, where photosynthesis and high temperatures favor excesses of oxygen. Seasonally alternating periods of oxygen exchanges in opposite directions would be expected in the temperate zones.

In addition, the flux climatology is seen to be generally consistent with a suite of independent data sets and models. Specifically, we find the following:

(1) Seasonal variations in the flux are consistent with seasonal variations in the atmospheric O_2/N_2 ratio, as simulated in two different atmospheric transport models [*Keeling et al.*, 1998; *Maloit*, 1998].

(2) Large-scale interbasin differences in the mean annual cycle of the biological component of the flux are qualitatively consistent with the primary productivity atlas of *Antoine et al.* [1996].

(3) The thermal and biological components of the air-sea oxygen flux are correlated, suggesting a relationship between heat flux and new production that is quantitatively consistent with observed surface phosphate-temperature relationships on the seasonal timescale.

(4) Spring/summer mixed layer new production, inferred from the biological air-sea oxygen flux in the extratropics, is quantitatively consistent with the drawdown of oxygen in the aphotic zone due to respiration during the same time period.

(5) Latitudinal and interbasin variations in the air-sea oxygen flux are qualitatively similar to those variations simulated by three-dimensional marine carbon cycle models, though there are significant differences in the Southern Ocean.

(6) The meridional oxygen transport inferred from the air-sea oxygen flux is consistent with transport estimates made from water mass analysis and inversion of hydrographic data in the Atlantic Ocean.

A secondary conclusion is that extratropical mixed layer new production estimated for the spring/summer period is 4.4-5.6 Gt C, with a corresponding f ratio of 0.38-0.46. Finally, we find that the estimates of seasonal net outgassing of *Keeling and Shertz* [1992] are too high by at least 100% in the Northern Hemisphere and 70% in the Southern Hemisphere.

Despite the overall consistency of the O_2 flux climatology with other independent data sets and models, there are a number of improvements that are needed if the climatology is to be used for finer-scale studies in addition to the basin-wide and global-scale analyses of the type made here. With few exceptions, the oxygen measurements are too sparse to be used very effectively for regional analyses of the mean annual cycle of the air-sea oxygen flux. Thus better coverage, particularly in the Southern Ocean is needed. A second area of improvement is in modeling the air-sea gas transfer velocity. This is needed particularly for making reliable estimates of the annual mean air-sea oxygen flux. The large sensitivity of meridional O_2 transport to the wind speed dependence of the transfer velocity highlights this difficulty. Third, models of bubble-induced O_2 supersaturation must be improved. The potential error here is quite large. For the models of the transfer velocity and bubble-induced supersaturation to be useful for large-scale analyses of the type made here, they must be able to exploit data sets available at global scales, such as those retrieved by satellite. Fourth, and finally, better understanding and quantification of the thermal skin effect and short-term covariances are needed in order to accurately assess their impacts on the air-sea oxygen flux.

Acknowledgments. We thank David Antoine for providing us with his primary production analyses. Reviews by Steve Emerson and Peter Brewer substantially improved the paper. This research was supported by the following awards: NASA 2383-MDIS/BGE005 and NSF Award OCE-9711937.

References

Anderson, L. A., and J. L. Sarmiento, Redfield ratios of remineralization determined by nutrient data analysis, *Global Biogeochem. Cycles*, *8*, 65-80, 1994.

Antoine, D., J.-M. André, and A. Morel, Oceanic primary production, 2, Estimation at global scale from satellite (coastal zone color scanner) chlorophyll, *Global Biogeochem. Cycles*, *10*, 57-70, 1996.

Archer, D., E. T. Peltzer, and D. L. Kirchman, A timescale for dissolved organic carbon production in equatorial Pacific surface water, *Global Biogeochem. Cycles*, *11*, 435-452, 1997.

Banse, K., and D. C. English, Seasonality of coastal zone color scanner phytoplankton pigment in the offshore ocean, *J. Geophys. Res.*, *99*, 7323-7345, 1994.

Bauer, S., G. L. Hitchcock, and D. B. Olson, Influence of monsoonally-forced Ekman dynamics upon surface layer depth and plankton biomass distribution in the Arabian Sea, *Deep Sea Res., Part A*, *38*, 531-553, 1991.

Bender, M., T. Ellis, P. Tans, R. Francey, and D. Lowe, Variability in the O_2/N_2 ratio of southern hemisphere air: Implications for the carbon cycle, *Global Biogeochem. Cycles*, *10*, 9-21, 1996.

Brewer, P. G., C. Goyet, and D. Dyrssen, Carbon dioxide transport by ocean currents at 25°N latitude in the Atlantic Ocean, *Science*, *246*, 477-479, 1989.

Capone, D. G., J. P. Zehr, H. W. Paerl, B. Bergman, and E. J. Carpenter, Trichodesmium, a globally significant marine cyanobacterium, *Science*, *276*, 1221-1229, 1997.

Conkright, M. E., S. Levitus and T. P. Boyer, *World Ocean Atlas 1994*, vol. 1, *Nutrients*, 150 pp., U.S. Dep. of Commer., Natl. Oceanic and Atmos. Admin., Washington, D.C., 1994.

Cornillon, P., and L. Stramma, The distribution of diurnal sea surface warming events in the Western Sargasso Sea, *J. Geophys. Res.*, *90*, 11,811-11,815, 1985.

Delnore, V. E., Diurnal variations of temperature and energy budget for the oceanic mixed layer during BOMEX, *J. Phys. Oceanogr.*, *2*, 239-247, 1972.

Deschamps, P. Y., and R. Frouin, Large diurnal heating of the sea surface observed by the HCMR experiment, *J. Phys. Oceanogr.*, *14*, 177-184, 1984.

Donlon, C. J., and I. S. Robinson, Observations of the oceanic thermal skin in the Atlantic Ocean, *J. Geophys. Res.*, *102*, 18,585-18,606, 1997.

Dugdale, R. C., and J. J. Goering, Uptake of new and regenerated forms of nitrogen in primary productivity, *Limnol. Oceanogr.*, *12*, 196-206, 1967.

Emerson, S., Seasonal oxygen cycles and biological new production in surface waters of the subarctic Pacific Ocean, *J. Geophys. Res.*, *92*, 6535-6544, 1987.

Emerson, S., P. Quay, C. Stump, D. Wilbur, and M. Knox, O_2, Ar, N_2 and ^{222}Rn in surface waters of the subarctic ocean: Net biological O_2 production, *Global Biogeochem. Cycles*, *5*, 49-69, 1991.

Emerson, S., P. Quay, C. Stump, D. Wilbur, and R. Schudlich, Determining primary production from the mesoscale oxygen field, *ICES Mar. Sci. Symp.*, *197*, 196-206, 1993.

Emerson, S., P. Quay, D. Karl, C. Winn, L. Tupas, and M. Landry, Experimental determination of the organic carbon flux from open-ocean surface waters, *Nature*, *389*, 951-954, 1997.

Eppley, R. W., and B. J. Peterson, Particulate organic matter flux and planktonic new production in the deep ocean, *Nature*, *282*, 677-680, 1979.

Falkowski, P. G., D. Ziemann, Z. Kolber, and P. K. Bienfang, Role of eddy pumping in enhancing primary production in the ocean, *Nature*, *352*, *55-58*, 1991.

Garcia, H. E., and L. I. Gordon, Oxygen solubility in seawater: Better fitting equations, *Limnol. Oceanogr.*, *37*, 1307-1312, 1992.

Gibson, J. K., P. Kallberg, S. Uppala, A. Hernandez, A. Nomura, and E. Serrano, ECMWF Re-Analysis Project Report Series, 1, ERA Description, European Cent. for Medium-Range Weather Forecasting, 72 pp., Reading, England, 1997.

Hansell, D. A., and C. A. Carlson, Net community production of dissolved organic carbon, *Global Biogeochem. Cycles, 12*, 443-453, 1998.

Hasse, L., The sea surface temperature deviation and the heat flow at the sea-air interface, *Boundary Layer Meteorol., 1*, 368-379, 1971.

Jenkins, W. J., and J. C. Goldman, Seasonal oxygen cycling and primary production in the Sargasso Sea, *J. Mar. Res., 43*, 465-491, 1985.

Keeling, R. F., and T.-H. Peng, Transport of heat, CO_2 and O_2 by the Atlantic's thermohaline circulation, *Philos. Trans. R. Soc. London, Ser. B, 348*, 133-142, 1995.

Keeling, R. F., and S. R. Shertz, Seasonal and interannual variations in atmospheric oxygen and implications for the global carbon cycle, *Nature, 358*, 723-727, 1992.

Keeling, R. F., R. G. Najjar, M. L. Bender, and P. P. Tans, What atmospheric oxygen measurements can tell us about the global carbon cycle, *Global Biogeochem. Cycles, 7*, 37-67, 1993.

Keeling, R. F., B. B. Stephens, R. G. Najjar, S. C. Doney, D. Archer, and M. Heimann, Seasonal variations in the atmospheric O_2/N_2 ratio in relation to the kinetics of air-sea gas exchange, *Global Biogeochem. Cycles, 12*, 141-164, 1998.

Levitus, S. and T. P. Boyer, *World Ocean Atlas 1994*, vol. 2, *Oxygen.* 172 pp., U.S. Dep. of Commer., Natl. Oceanic and Atmos. Admin., Washington, D.C., 1994a.

Levitus, S., and T. P. Boyer, *World Ocean Atlas 1994*, vol. 4, *Temperature,* 117 pp., U.S. Dep. of Commer., Natl. Oceanic and Atmos. Admin., Washington, D.C., 1994b.

Levitus, S., R. Burgett, and T. P. Boyer, *World Ocean Atlas 1994*, vol. 3, *Salinity,* 99 pp., U.S. Dep. of Commer., Natl. Oceanic and Atmos. Admin., Washington, D.C., 1994.

Liss, P. S., and L. Merlivat, Air-sea gas exchange rates: Introduction and synthesis, in *The Role of Air-Sea Exchange in Geochemical Cycling*, edited by P. Buat Menard, pp. 113-127, D. Reidel, Norwell, Mass., 1986.

MacDonald, A. M., Property fluxes at 30°S and their implications for the Pacific-Indian throughflow and the global heat budget, *J. Geophys. Res., 98*, 6851-6868, 1993.

Maloit, P. F., Variations in the atmospheric oxygen-to-nitrogen ratio due to air-sea exchange: Simulations with the GENESIS general circulation model, Masters thesis, 53 pp., Penn. State Univ., University Park, 1998.

Martel, F., and C. Wunsch, The North Atlantic circulation in the early 1980s—An estimate from inversion of a finite difference model, *J. Phys. Oceanogr., 23*, 898-924, 1993.

Najjar, R. G., and R. F. Keeling, Analysis of the mean annual cycle of the dissolved oxygen anomaly in the World Ocean, *J. Mar. Res., 55*, 117-151, 1997.

Oudot, C., O_2 and CO_2 balances approach for estimating biological production in the mixed layer of the tropical Atlantic Ocean (Guinea Dome area), *J. Mar. Res., 47*, 386-409, 1989.

Price, J. F., R. A. Weller, and R. Pinkel, Diurnal cycling: Observations and models of the upper ocean response to diurnal heating, cooling, and wind mixing, *J. Geophys. Res., 91*, 8411-8427, 1986.

Price, J. F., R. A. Weller, C. M. Bowers and M. G. Briscoe, Diurnal response of sea surface temperature observed at Long-Term Upper Ocean Study (34°N, 70°W) in the Sargasso Sea, *J. Geophys. Res., 92*, 14,480-14,490, 1987.

Ravier-Hay, P., and J. S. Godfrey, A model of diurnal changes in sea surface temperature for the Western Equatorial Pacific Ocean, *TOGA Notes, April,* 5-8, 1993.

Redfield, A. C., The exchange of oxygen across the sea surface, *J. Mar. Res., 7*, 347-361, 1948.

Richards, F. A., Oxygen in the ocean, *Mem., Geol. Soc. America, 57*, 185-238, 1957.

Rintoul, S., and C. Wunsch, Mass, heat, oxygen and nutrient fluxes and budgets in the North Atlantic Ocean, *Deep-Sea Res. 38, Part A, suppl. 1*, S355-S377, 1991.

Roach, A. T., K. Aagaard, C. H. Pease, S. A. Salo, T. Weingartner, V. Pavlov, and M. Kulakov, Direct measurements of transport and water properties through the Bering Strait, *J. Geophys. Res., 100*, 18,433-18,457, 1995.

Robertson, J. E., A. J. Watson, C. Langdon, R. D. Ling, and J. W. Wood, Diurnal variation in surface pCO_2 and O_2 at 60°N and 20°W in the North Atlantic, *Deep Sea Res., Part II, 40*, 409-422, 1993.

Sarmiento, J. L. S., and E. T. Sundquist, Revised budget for the oceanic uptake of anthropogenic carbon dioxide, *Nature, 356*, 589-593, 1992.

Saunders, P. M., and B. A. King, Oceanic fluxes on the WOCE A11 Section, *J. Phys. Oceanogr., 25*, 1942-1958, 1995.

Shea, D. J., K. E. Trenberth, and R. W. Reynolds, A global monthly sea surface temperature climatology, *J. Clim., 5*, 987-1001, 1992.

Spitzer, W. S., and W. J. Jenkins, Rates of vertical mixing, gas exchange and new production: Estimates from seasonal gas cycles in the upper ocean near Bermuda, *J. Mar. Res., 47*, 169-196, 1989.

Stephens, B. B., R. F. Keeling, M. Heimann, K. D. Six, R. Murnane, and K. Caldeira, Testing global ocean carbon cycle models using measurements of atmospheric O_2 and CO_2 concentration, *Global Biogeochem. Cycles, 12*, 213-230, 1998.

Takahashi, T., J. Olafsson, J. G. Goddard, D. W. Chipman, and S. C. Sutherland, Seasonal variations of CO_2 and nutrients in the high-latitude surface oceans: a comparative study, *Global Biogeochem. Cycles, 7*, 843-878, 1993.

Takahashi, T., R. A. Feely, R. Weiss, R. H. Wanninkhof, D. W. Chipman, S. C. Sutherland, and T. T. Takahashi, Global air-sea flux of CO_2: An estimate based on measurements of air-sea pCO_2 difference, *Proc. Nat. Acad. Sci. U.S.A., 94*, 8292-8299, 1997.

Tans, P. P., I. Y. Fung, and T. Takahashi, Observational constraints on the global atmospheric CO_2 budget, *Science, 247*, 1431-1438, 1990.

Wanninkhof, R., Relationship between wind speed and gas exchange over the ocean, *J. Geophys. Res., 97*, 7373-7382, 1992.

Wick, G. A., W. J. Emery, and L. H. Kantha, The behavior of the bulk-skin temperature difference under varying wind speed and heat flux, *J. Phys. Oceanogr., 26*, 1969-1988, 1996.

Wyrtki, K., An estimate of equatorial upwelling in the Pacific, *J. Phys. Oceanogr., 11*, 1205-1214, 1981.

Yoder, J. A., C. R. McClain, G. C. Feldman, and W. E. Esaias, Annual cycles of phytoplankton chlorophyll concentrations in the global ocean: A satellite view, *Global Biogeochem. Cycles, 7*, 181-194, 1993.

R. F. Keeling, Scripps Institution of Oceanography, 9500 Gilman Drive, Dept. 0236, La Jolla, CA 92093 (rkeeling@ucsd.edu)

R. G. Najjar, Department of Meteorology, Pennsylvania State University, University Park, PA 16802. (najjar@essc.psu.edu)

(Received August 24, 1998; revised March 8, 1999;
accepted April 29, 1999).